Collision-Tolerant Narrowband Communication using Non-Orthogonal Modulation and Multiple Access

Chin-Wei Hsu, Hun-Seok Kim, *Member, IEEE*
Department of EECS, University of Michigan, Ann Arbor, MI
chinweih@umich.edu, hunseok@umich.edu

***Abstract*—Ultra Narrowband (UNB) has recently received great attention for its potential to realize ultra-reliable, massive scale Low Power Wide Area Networks (LPWAN). Elaborate frequency planning and multiple access schemes have been regarded as an essential part of LPWAN because random frequency- and time-domain ALOHA accesses lead to significant network performance degradation due to inevitable packet collisions. In this paper, we propose a novel network scheme based on non-orthogonal modulation and multiple access (NOMMA) that is tolerant to packet collisions. The proposed scheme uses hyper-dimensional modulation (HDM) to outperform conventional orthogonal modulation and multiple access schemes with and without prior knowledge of interference in highly congested network scenarios. Simulation results show that HDM based NOMMA can achieve 70% higher network throughput than a conventional orthogonal modulation and multiple access scheme.**

I. Introduction

Massive deployment of Internet of Things (IoT) enables new applications that can dramatically change our daily life. Toward realization of the massive IoT concept, a new class of Low Power Wide Area Network (LPWAN) is recently gaining significant attention [1]. LPWAN enables communication among low-cost terminal devices over kilometers distance, sustaining very long lifetime (several years) with a single cell battery. This kind of communication requires novel physical layer and multiple access schemes that can support a large number of low power devices that exchange relative low data rate messages in a wide coverage area. For LPWAN, spread spectrum and ultra narrowband (UNB) solutions are proposed to achieve sensitivity as low as -130 dBm. LoRa [2] is based on spread spectrum while Sigfox [3] uses UNB modulations.

UNB is one of the most promising LPWAN techniques for several reasons [4]. One main advantage is that UNB allows devices to operate at very low received signal power as reducing the bandwidth leads to lower noise power which is proportional to the bandwidth. Another benefit of UNB is that the maximum number of concurrently transmitting nodes can be very high because each node only occupies very limited bandwidth. Ultra-narrow bandwidth occupancy allows relatively low carrier frequency (typically sub-1GHz) for reduced pathloss and also lower transceiver power consumption.

This work was funded by the DARPA YFA #D18AP00076.

While UNB provides many advantages, it also raises unique issues [5]. Carrier frequency synchronization becomes critical when the transmission bandwidth is very narrow. Frequency uncertainty may extend over multiple times of the signal bandwidth. For example, a low cost crystal with 50ppm accuracy results in 50kHz frequency offset for the 1GHz carrier frequency, which is substantial for an UNB scheme that often operates with $\leq$1kHz bandwidth. To filter out-of-band noise while capturing the full in-band signal power, very tight synchronization of the carrier frequency is needed.

A star network topology with an ALOHA based random access scheme is often considered in LPWANs [6]. ALOHA in time domain has been studied for decades and it is well known that time domain collisions can severely degrades the network capacity unless a proper interference handling scheme is employed [7]. Random channel resource allocation for ALOHA can be extended to frequency domain by allowing each node to transmit at a random carrier frequency without a strict sub-channel definition. In that case, the carrier frequency of a transmitted packet can be continuously and uniformly distributed in the overall spectrum. As a consequence of this pure ALOHA, packet collisions are inevitable in both time and frequency domain when the number of deployed nodes is large in a wide area.

Many prior works have investigated the interference issue caused by packet collisions in ALOHA access schemes for UNB [5], [8]–[13]. While they assume different scenarios and network schemes, most of them use a simplified packet error rate (PER) model to analyze the impact of inter-packet interference. For example, [5], [8], [9] assume that the packet is lost whenever there is a collision in time or frequency domain, which is too pessimistic if the interference power is low compared to the desired packet and a strong error correction code is employed. In [10]–[12], PER is defined as the probability of an event where a packet does not meet a certain signal-to-interference noise ratio (SINR) threshold, which is a reasonble model when the channel is frequency non-selective. Prior work [13] analyzes the PER through empirical results but packet-level successive interference cancellation (SIC) [14] is not performed to mitigate packet collisions. On the contrary, in this paper we demonstrate and quantify the enhanced network performance in a pure ALOHA scenario where time and

978-1-7281-0962-6/19/$31.00 ©2019 IEEE

frequency collisions are efficiently mitigated using a hyper-dimensional modulation (HDM) based non-orthogonal modulation [15] and multiple access scheme (NOMMA) combined with packet-level SIC.

To enhance network performance of UNB LPWAN, we propose a new HDM [15] based NOMMA, where frequency and time domain packet collisions from pure ALOHA accesses are liberally allowed and mitigated at the gateway. To exploit the full advantage of NOMMA, we demonstrate that the interference power level and arrival timing information is critical for the decoding process at the gateway. Through extensive simulations, HDM based NOMMA is shown to outperform conventional schemes in an LPWAN in terms of network PER and throughput.

II. Ststem Model

A. Transmission Model

We consider an UNB uplink star network with multiple transmit nodes and one receiver gateway. Let M be the total node number in the network. The received signal at the gateway at time t can be expressed as

$$y(t) = \sum_{m=1}^{M} h_m \cdot \big(\tilde{x}_m(t) * p(t)\big) e^{j2\pi f_m t} + \tilde{w}(t) \qquad (1)$$

where y is the received signal and $\tilde{w}$ is the additive Gaussian noise. The transmitted signal $\tilde{x}_m(t) = \sum_n x_m[n]\delta(t - nT)$ is obtained from the discrete sample $x_m[n]$ while $\delta(t)$ denotes the delta function and T is the sampling interval. The bandwidth (BW) of the modulated signal is defined as $BW = 1/T$. $p(t)$ is a pulse shaping function and $*$ denotes convolution. f_m denotes the carrier frequency of node m and h_m represents a complex channel coefficient which is constant (flat) for a packet with a narrow bandwidth assumption.

To demodulate a packet from node m, we assume the gateway has perfect information of the channel and carrier frequency. The gateway first down-converts the signal according to the carrier frequency f_m, then applies a low pass filter (LPF) to the baseband signal. Matched filtering with $p(t)$ is performed before sampling at the correct timing. Resulting received samples can be expressed as

$$r_m[n] = \big(\text{LPF}\{y(t)e^{-j2\pi f_m t}\} * p(t)\big)\Big|_{t=nT} \qquad (2)$$

$$= h_m \cdot x_m[n] + z_m[n] + w[n] \qquad (3)$$

or, by using a vector notation for the entire packet,

$$\mathbf{r}_m = h_m \mathbf{x}_m + \mathbf{z}_m + \mathbf{w} \qquad (4)$$

where $\mathbf{z}_m$ denotes the interference from other nodes and $\mathbf{w}$ denotes the discrete additive Gaussian noise in baseband. In following sections we use (4) as our signal model.

The interference $\mathbf{z}_m$ can be ignored when there are no other packets transmitted at the same time or the carrier frequency is far enough from f_m. In this paper, we mainly focus on a random ALOHA access network with a large number of nodes where collisions occur frequently and thus become the limiting factor for the network performance.

B. Collision in frequency and time domain

The packet collision is an event where two or more packets overlap with each other in time and frequency domain. Overlapping in frequency is often defined by assuming each packet occupies a fixed bandwidth ($BW = 1/T$) as illustrated in Figure 1. As packet collisions often cause packet errors, some prior works such as [5], [8], [9] declare that a packet is lost for any collision while some [10]–[12] calculate the packet signal to interference ratio (SINR) based on severity of collision to claim that a packet is lost when its SINR is below a predefined threshold. However, in realistic cases, not all collisions result in packet error and SINR alone is not a sufficient metric to determine the PER.

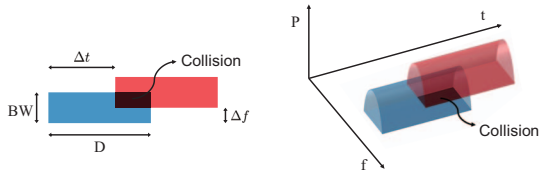

Fig. 1: Collision in time and frequency domain (2D and 3D)

When a collision occurs, symbol SINR degradation is determined by interfering packets' power and frequency distance from the desired packet. According to [11], the interference power density for UNB networks can be approximated by a zero-mean Gaussian function:

$$\beta(\Delta f) = \frac{A}{\sigma\sqrt{2\pi}} e^{-\frac{\Delta f^2}{2\sigma^2}} \qquad (5)$$

where Δf is the carrier frequency offset between the desired packet and the interfering packet. A and σ depend on the system parameters such as LPF specification for baseband processing. Figure 2 shows the simulated interference power after LPF and the approximated model for a scenario where unit power BPSK single carrier modulation is used for the desired packet and interference, $BW = 1/T = 1$kHz, LPF has passband of 1kHz, and stopband of 2kHz with stopband attenuation of 45dB. It confirms the model with the parameter $A = 841$ and $\sigma = 428$ for this scenario is quite accurate at the frequency offset where the interference power is not negligible.

Analyzing the PER for packet collision scenarios is complicated when the packet is encoded with a strong error correction code (FEC) and SIC is adopted. While the total packet interference power can be modeled by (5) and scaling it according to the overlapping length in time, the PER performance cannot be simply derived from the resulting packet SINR when a strong FEC such as low-density parity check (LDPC) or polar code is applied. Furthermore, FEC decoding algorithms typically operate on log-likelihood ratio (LLR) as their decoder input and LLR calculation for each symbol requires knowledge on the interference packet power level, collision timing, and probability density function of the interfering signal.

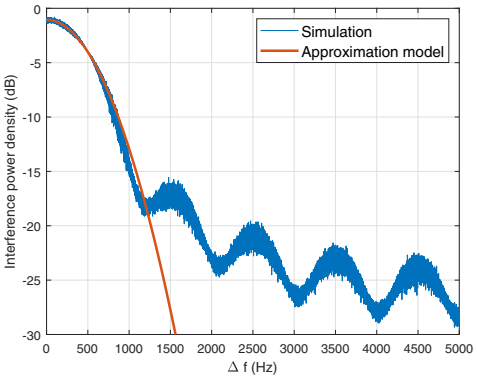

Fig. 2: Interference power density model simulation vs. approximation.

The performance metric used in this paper is the empirical average network PER and network throughput. We assume that each packet arrives following a Poisson process with a uniformly distributed random carrier frequency within a range of (f_{min}, f_{max}), where $f_{max} - f_{min} \gg BW$ so that the boundary effect can be neglected.

III. Proposed HDM based NOMMA

To alleviate the performance degradation from packet collisions in pure ALOHA networks, we propose hyper-dimensional modulation (HDM) based non-orthogonal modulation and multiple access (NOMMA). In this section we show the impact of packet collision to HDM with or without information of interference power level and timing.

A. HDM without interference knowledge

HDM is a recently proposed modulation scheme [15] where multiple information symbols are non-orthogonally combined and modulated with a hyper-dimenional vector through a fast linear transformation and random permutation. The modulation process of HDM can be expressed as

$$\mathbf{x} = \sum_{v=1}^{V} \mathbf{P}_v \mathcal{F}(\mathbf{x}_v) \tag{6}$$

where $\mathbf{x}$ is the transmitted signal vector (packet) with a dimension of $D \times 1$, $\mathbf{P}_v$ denotes a random permutation matrix and $\mathcal{F}$ is a fast linear transform such as fast Fourier transform (FFT) or fast Walsh Hadamard transform (FWHT). $\mathbf{x}_v \in \mathbb{C}^D$ is a sparse vector that contains information modulated by both pulse position modulation (PPM) and phase-shift keying (PSK). Through the fast linear transform and permutation, a sparse vector $\mathbf{x}_v$ is transformed to a non-sparse random vector, which is nearly orthogonal to other vectors $\mathbf{x}_{v'}$ that are added to $\mathbf{x}$ when the dimension D is sufficiently large. These V vectors are added together to form an HDM packet $\mathbf{x}$ of length D whose element is sequentially transmitted as a discrete sample. It is shown in [15] that uncoded HDM's PER performance is comparable to that of LDPC and polar coded BPSK modulation with the same spectral efficiency for a relatively short packet ($D = 256$).

To demodulate an HDM packet, an iterative SIC algorithm is used [15]. At the beginning of each iteration, intra-packet interference is cancelled with the result of the previous iteration. The received signal after SIC can be expressed as

$$\mathbf{y}_v = \mathbf{r} - \sum_{u \neq v} \mathbf{P}_u \mathcal{F}(\hat{\mathbf{x}}_u) \tag{7}$$

where $\mathbf{r}$ is the received vector after channel equalization and $\mathbf{y}_v$ is the vector after SIC for the original vector $\mathbf{x}_v$. Inverse permutation and inverse fast linear transformation are then applied to get the estimate $\hat{\mathbf{x}}_v$ for each stream using (8).

$$\hat{\mathbf{x}}_v = \mathcal{F}^{-1}(\mathbf{P}_v^{-1}\mathbf{y}_v) \tag{8}$$

Finally, the information of each stream can be estimated through a low-complexity maximum-likelihood algorithm exploiting the sparsity of $\mathbf{x}_v$ (PPM modulated). The iteration continues until convergence or a predetermined number of iterations is reached. At the end of demodulation, a CRC-based error correction is performed to further decrease the PER with details provided in [15].

HDM is robust to packet collisions because of its unique modulation structure. During the demodulation process, interference introduced by partial packet overlaps in time is spread to all samples because of the fast linear transform and permutation. That is, every symbol in a packet is equally corrupted by the same amount of interference power. This *interference spreading* is particularly helpful for reducing PER when the information of interference power level and timing is unknown. Unlike FEC protected conventional modulations, the impact of unknown collision will simply translate to the same average SINR loss to all symbols in an HDM packet. On the contrary, unknown partial collisions in a conventional BPSK modulation results in unequal (and unknown) LLR degradation for each symbol that can cause significant degradation of FEC.

B. HDM with interference knowledge

When the knowledge of interference is obtainable, it can significantly enhance the PER performance for both HDM and a conventional modulation with FEC. For HDM, an MMSE estimator of the transmit signal $\mathbf{x}$ in (6) can be applied before passing it to the inverse process in (7) and (8) when the covariance matrix of the interference plus noise is known. For the covariance calculation, the knowledge of interference power level and timing is required. The MMSE estimate of $\mathbf{x}$ can be expressed as

$$\mathbf{r}_{\text{mmse}} = (\mathbf{I} + \frac{1}{P_S}\mathbf{C}_\mathbf{z})^{-1}\mathbf{r} = \mathbf{\Lambda}(\mathbf{x} + \mathbf{z} + \mathbf{w}) \tag{9}$$

where P_S denotes the power of the transmitted signal and $\mathbf{C}_\mathbf{z}$ is the interference plus noise covariance matrix. $\mathbf{C}_\mathbf{z} = \mathbf{E}\{(\mathbf{z} + \mathbf{w})(\mathbf{z} + \mathbf{w})^H\}$ and $\mathbf{\Lambda} = (\mathbf{I} + \frac{1}{P_S}\mathbf{C}_\mathbf{z})^{-1}$ are both diagonal.

The linear MMSE processing of $\mathbf{\Lambda}$ can be applied right before the inverse process (8), thus the SIC stage is not affected by the MMSE processing. The MMSE inverse process is modified to

$$\hat{\mathbf{x}}_v = \mathcal{F}^{-1}(\mathbf{P}_v^{-1}\mathbf{\Lambda}\mathbf{y}_v). \tag{10}$$

Since $\mathbf{C_z}$ and $\mathbf{\Lambda}$ are both diagonal, MMSE processing does not incur significant overhead for HDM demodulation.

MMSE processing effectively suppresses the contribution of samples that are corrupted by strong interference. Similarly, applying interference knowledge to the LLR computation of conventional modulation results in small LLR values for symbols that are corrupted by interference. Performance comparison between uncoded HDM and polar coded BPSK with interference knowledge is provided in Section IV.

C. HDM PER under collision

For HDM, interference from partial collision is spread over the entire packet, resulting in the same SINR for all symbols in the packet. Calculating the exact PER for HDM is difficult because of SIC and CRC based error correction. Instead, in this paper, we analyze the packet effective SINR under partial collision and show that it can be directly used to infer the PER, thus can be a performance indicator of an HDM packet.

When the carrier frequency difference Δf is known for a packet collision, the interference plus noise covariance matrix $\mathbf{C_z}$ can be obtained by

$$[\mathbf{C_z}]_{i,i} = \sum_{k\in\mathcal{I}} P_k \beta(\Delta f_k) + N_0 \tag{11}$$

where $\mathcal{I}$ denotes the set of the packets collided with the i_{th} sample of the desired packet, P_k is the power of the interference packet, and Δf_k is the frequency difference.

For HDM without interference knowledge, the SINR can then be calculated as

$$\text{SINR}_{\text{zf}} = \frac{P_S}{\text{tr}(\mathbf{C_z})}. \tag{12}$$

Whereas when interference knowledge is available, the effective SINR for HDM MMSE demodulation can be derived from the error of the MMSE estimator. The MMSE estimator in (10) can be expressed as

$$\hat{\mathbf{x}}_v = \mathbf{W}^H\mathbf{P}_v^H\mathbf{\Lambda}\mathbf{P}_v\mathbf{W}\mathbf{x}_v + \mathbf{e}_v \tag{13}$$

where $\mathbf{W}$ is the fast linear transform matrix whose inverse is its Hermitian $\mathbf{W}^H$ and $\mathbf{e}_v = \mathbf{W}^H\mathbf{P}_v^H\mathbf{\Lambda}(\mathbf{z}+\mathbf{w})$ denotes the error. The covariance matrix of the error vector is obtained by

$$\mathbf{C_e} = \mathbf{W}^H\mathbf{P}_v^H\mathbf{\Lambda}\mathbf{C_z}\mathbf{\Lambda}\mathbf{P_v}\mathbf{W} \tag{14}$$

$$= \mathbf{W}^H\mathbf{\Sigma}\mathbf{W}^H \tag{15}$$

where $\mathbf{\Sigma} = \mathbf{P}_v^H\mathbf{\Lambda}\mathbf{C_z}\mathbf{\Lambda}\mathbf{P}_v$ is a diagonal matrix. Note that when FFT is used for $\mathbf{W}$, $\mathbf{C_e}$ becomes a circulant matrix that has the same diagonal values. From (13) and (15), the unbiased SINR can be calculated as

$$\text{SINR}_{\text{mmse}} = \frac{P_S \cdot \left(\sum_i \frac{P_S}{P_S+\sigma_i}\right)^2}{D \cdot \sum_i \sigma_i (\frac{P_S}{P_S+\sigma_i})^2} \tag{16}$$

where σ_i represents the i-th diagonal element of $\mathbf{C_z}$.

Note that the actual PER performance of the HDM under collisions is slightly different from that in an additive white Gaussian noise (AWGN) channel with the same S(I)NR. The reason is that the entries in the error vector is correlated, affecting the probability of an error event in SIC. Nevertheless, the SINR derivation is still useful as an accurate indicator for PER estimation as all HDM samples experience the same SINR. When the number of corrupted samples by interference is large, correlation becomes small and thus the PER performance is accurately estimated by substituting the calculated SINR with the SNR in AWGN (no collision case).

D. NOMMA

Combining HDM with ALOHA based non-orthogonal multiple access with random (overlapping) frequency allocation, we propose NOMMA to enhance network performance. As we assume an uplink scenario where numerous low power nodes are totally unsynchronized both in time and frequency, a more advanced code-domain non-orthogonal multiple access (NOMA) scheme such as sparse code multiple access [16] that require time and frequency synchronization is not considered in this work. Allowing a random carrier frequency is particularly beneficial for a low power ultra narrowband node where accurate carrier frequency control with respect to the narrow bandwidth can be challenging given the low complexity constraint. We assume the gateway is capable of monitoring the entire frequency range to detect an UNB packet at an arbitrary time and frequency using a powerful algorithm that uses multiple hypotheses [17]. HDM is particularly advantageous for the proposed NOMMA as it allows the gateway to handle partial collisions in a more robust way even if it cannot acquire the full knowledge of the interference.

It is well known that applying inter-packet SIC between collided packets significantly improves the network performance in terms of capacity or PER [14]. Therefore, for the proposed NOMMA, we assume a gateway always performs inter-packet SIC after successfully decoding a packet by checking the CRC. The NOMMA network system is illustrated in Fig. 3.

We consider two scenarios with and without interference knowledge. The first scenario is when the knowledge of interference cannot be obtained. The gateway always decodes the earlier arriving packet immediately without knowing later arriving packets causing collisions. Power and timing of interfering packets are unknown. Successfully decoded packets are immediately cancelled after successful demodulation, exposing later arriving interference packets for sequential processing. The second scenario assumes that the gateway can acquire power and timing knowledge for all interference packets as packet detection is performed before starting SIC demodulation process for each packet. In this case, the covariance of interference is known and used in the demodulation.

IV. Evaluation

The performance of the proposed HDM based NOMMA is evaluated via extensive Monte-Carlo computer simulations.

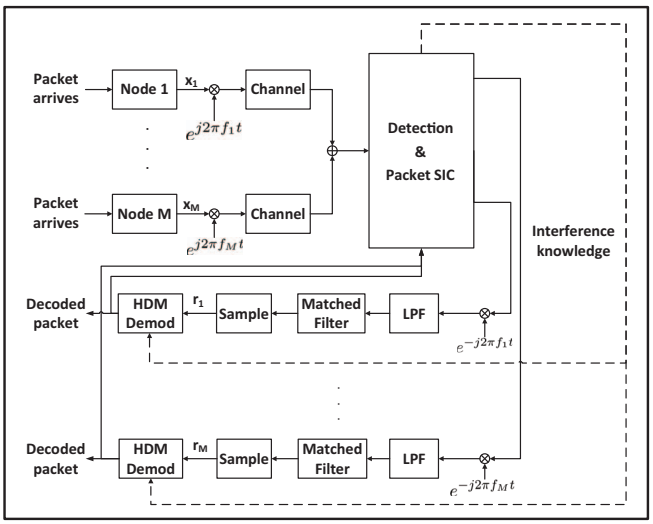

Fig. 3: Proposed NOMMA network diagram

We choose a packet length of $D = 256$ samples for UNB applications where each node communicates short messages at a low rate for long distance uplink. Uncoded HDM modulation parameters are selected to have a modulation rate or spectral efficiency of 0.5078 bit/s/Hz with $D = 256$.

Fig. 4 shows the PER of HDM with and without interference knowledge. To demonstrate the influence of $\mathbf{C_z}$ on PER, we fix tr($\mathbf{C_z}$), while changing the diagonal component as

$$[\mathbf{C_z}]_{i,i} = \begin{cases} 0 & \text{for} \quad i \leq D - b \\ P_z/b & \text{for} \quad i > D - b \end{cases}$$

with varying b where b is the length of two packet collision in samples and P_z denotes the total interference power. As discussed by the analysis in Section III.C, the PER performance is governed by the effective SINR.

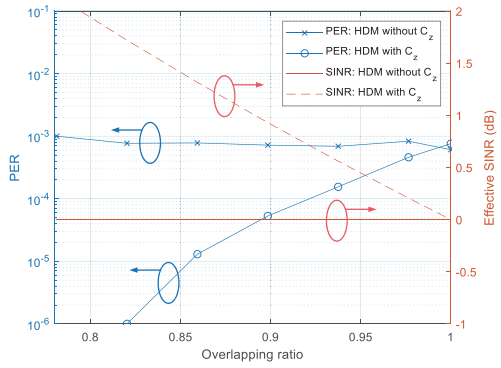

Fig. 4: PER performance of HDM under collision

We compare uncoded HDM to conventional BPSK modulation with 1/2 rate polar coding for the same 256-bit length packet. Note that polar-coded BPSK and uncoded HDM have a similar BER with less than 0.5dB difference in AWGN. LDPC has worse performance than polar for a short packet, thus we exclude it from comparison. We use a matched spectral efficiency of 0.5 bit/s/Hz for both uncoded HDM and polar coded BPSK. For LLR calculation for polar code, we assume complex Gaussian random samples for the interference which becomes valid when many packets collide on top of each other.

Figure 5 shows the PER comparison between HDM and polar coded BPSK when an interfering packet with complex Gaussian random samples collides with the desired packet with varying power and overlapping ratio (1.0 is full collision). SNR without collision is set to 3dB for Fig. 5. One can see that applying interference knowledge for $\mathbf{C_z}$ and LLR computation is critical to the PER performance. Uncoded HDM exhibits lower PER than polar coded BPSK, and has significant gain with interference knowledge. It confirms that, to satisfy a certain PER threshold, HDM can tolerate significantly higher power interference and/or longer time overlapping.

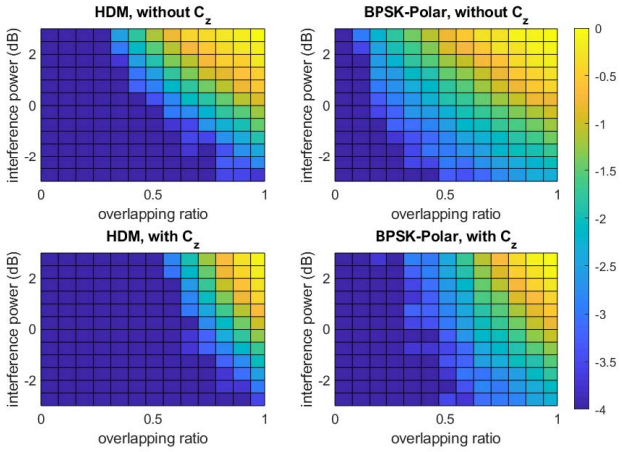

Fig. 5: PER of HDM vs. BPSK-Polar under interference with varying power and time overlapping. PER is shown in log scale with colors.

Next, we simulate a NOMMA network to evaluate its network average PER and throughput for an equal power packet collision scenario. All packets arrived at the gateway are assumed to have the same power, corresponding to a case where all transmitter nodes perform perfect power control to maintain a target SNR. We set the SNR to 3dB, which is relatively low so that LPWAN operates with a robust modulation scheme such as HDM or polar coded BPSK. Note that this equal packet power scenario is a worst case scenario to perform inter-packet SIC at the gateway as the power difference between packets is small.

Figure 6 shows the average network PER for various network load of λ in bit/s/Hz. Note that λ can be mapped to an equivalent active number of nodes in a network. In an orthogonal multiple access (OMA) case, orthogonal channel carrier frequencies are separated by $BW = 1/T$ Hz so that the interference from adjacent channels become negligible. Also packets in OMA are transmitted using a time slot globally synchronized and whose length is equal to the packet length ($D = 256$) so that packets do not overlap at all or

completely overlap when they use the same resource block (i.e., combination of a time slot and frequency channel). In the OMA case, HDM and BPSK-Polar have similar performance because the collision probability to use the same orthogonal resource block limits the PER. Whereas when pure ALOHA in time and frequency is adopted, both HDM and BPSK-Polar outperforms OMA thanks to strong interference mitigation property of HDM or robust polar based FEC for BPSK to combat corrupt samples. While both schemes significantly benefit from the knowledge of interference $\mathbf{C_z}$, observe that NOMMA with HDM exhibits a larger gain compared to BPSK-Polar.

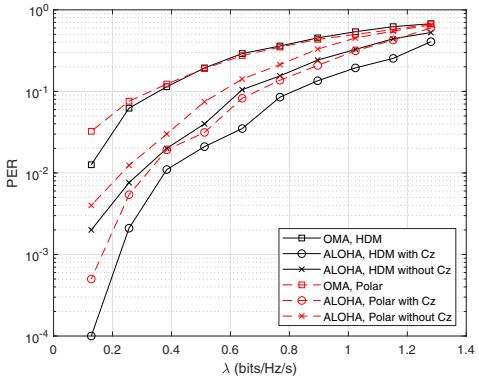

Fig. 6: Network PER with equal power packets

Figure 7 shows the network throughput given different network loads of λ in bit/s/Hz. The network throughput is calculated by Throughput$(\lambda) = \lambda(1-\text{PER}(\lambda))$ where PER(λ) is empirically obtained from simulations. Figure 7 shows that HDM based NOMMA can achieve a significantly higher throughput than BPSK-Polar in a pure ALOHA case. The largest gain from HDM based NOMMA is up to 20% and 70% higher throughput compared to BPSK-Polar based non-orthogonal multiple access and OMA schemes respectively.

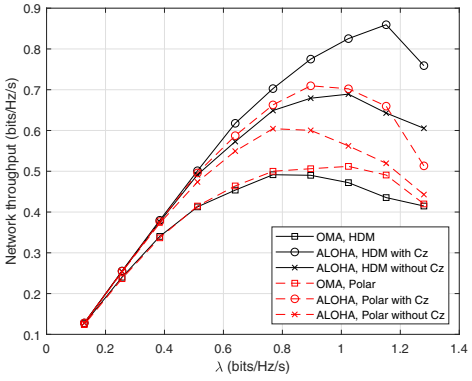

Fig. 7: Network throughput with equal power packets

V. Conclusion

In this paper, we proposed a HDM based NOMMA for LPWAN to combat packet collisions for enhanced network performance. The impact of collisions in frequency and time domain on PER was discussed and we demonstrated a decoding algorithm to use the interference knowledge to reduce the PER. We demonstrated that an HDM-based NOMMA exhibits superior collision-tolerance compared to a conventional scheme in terms of network PER and throughput. It exhibits a 20 – 70% gain over conventional schemes that are based on polar-coded BPSK NOMA and OMA.

References

[1] U. Raza, P. Kulkarni, and M. Sooriyabandara, "Low power wide area networks: An overview," *IEEE Communications Surveys Tutorials*, vol. 19, no. 2, pp. 855–873, Secondquarter 2017.

[2] L. Alliance, April 2019. [Online]. Available: https://lora-alliance.org/

[3] Sigfox, April 2019. [Online]. Available: https://www.sigfox.com/

[4] W. Yang, M. Wang, J. Zhang, J. Zou, M. Hua, T. Xia, and X. You, "Narrowband wireless access for low-power massive internet of things: A bandwidth perspective," *IEEE Wireless Communications*, vol. 24, no. 3, pp. 138–145, June 2017.

[5] M. Anteur, V. Deslandes, N. Thomas, and A. Beylot, "Ultra narrow band technique for low power wide area communications," in *2015 IEEE Global Communications Conference (GLOBECOM)*, Dec 2015, pp. 1–6.

[6] X. Xiong, K. Zheng, R. Xu, W. Xiang, and P. Chatzimisios, "Low power wide area machine-to-machine networks: key techniques and prototype," *IEEE Communications Magazine*, vol. 53, no. 9, pp. 64–71, Sep. 2015.

[7] S. M. R. Islam, N. Avazov, O. A. Dobre, and K. Kwak, "Power-domain non-orthogonal multiple access (noma) in 5g systems: Potentials and challenges," *IEEE Communications Surveys Tutorials*, vol. 19, no. 2, pp. 721–742, Secondquarter 2017.

[8] B. Vejlgaard, M. Lauridsen, H. Nguyen, I. Z. Kovacs, P. Mogensen, and M. Sorensen, "Interference impact on coverage and capacity for low power wide area iot networks," in *2017 IEEE Wireless Communications and Networking Conference (WCNC)*, March 2017, pp. 1–6.

[9] Z. Li, S. Zozor, J. Brossier, N. Varsier, and Q. Lampin, "2d time-frequency interference modelling using stochastic geometry for performance evaluation in low-power wide-area networks," in *2017 IEEE International Conference on Communications (ICC)*, May 2017, pp. 1–7.

[10] G. Hattab and D. Cabric, "Spectrum sharing protocols based on ultra-narrowband communications for unlicensed massive iot," in *2018 IEEE International Symposium on Dynamic Spectrum Access Networks (DySPAN)*, Oct 2018, pp. 1–10.

[11] Y. Mo, C. Goursaud, and J. Gorce, "Theoretical analysis of unb-based iot networks with path loss and random spectrum access," in *2016 IEEE 27th Annual International Symposium on Personal, Indoor, and Mobile Radio Communications (PIMRC)*, Sep. 2016, pp. 1–6.

[12] ——, "On the benefits of successive interference cancellation for ultra narrow band networks : Theory and application to iot," in *2017 IEEE International Conference on Communications (ICC)*, May 2017, pp. 1–6.

[13] M. Anteur, V. Deslandes, N. Thomas, and A. Beylot, "Modeling and performance analysis of ultra narrow band system for m2m," in *2016 8th Advanced Satellite Multimedia Systems Conference and the 14th Signal Processing for Space Communications Workshop (ASMS/SPSC)*, Sep. 2016, pp. 1–6.

[14] X. Zhang and M. Haenggi, "The performance of successive interference cancellation in random wireless networks," *IEEE Transactions on Information Theory*, vol. 60, no. 10, pp. 6368–6388, Oct 2014.

[15] H. Kim, "Hdm: Hyper-dimensional modulation for robust low-power communications," in *2018 IEEE International Conference on Communications (ICC)*, May 2018, pp. 1–6.

[16] H. Nikopour and H. Baligh, "Sparse code multiple access," in *2013 IEEE 24th Annual International Symposium on Personal, Indoor, and Mobile Radio Communications (PIMRC)*, Sep. 2013, pp. 332–336.

[17] Y. Chen, N. Chiotellis, L. Chuo, C. Pfeiffer, Y. Shi, R. G. Dreslinski, A. Grbic, T. Mudge, D. D. Wentzloff, D. Blaauw, and H. S. Kim, "Energy-autonomous wireless communication for millimeter-scale internet-of-things sensor nodes," *IEEE Journal on Selected Areas in Communications*, vol. 34, no. 12, pp. 3962–3977, Dec 2016.